

Dielectric relaxation study of the dynamics of monosaccharides: D-ribose and 2-deoxy-D-ribose

This article has been downloaded from IOPscience. Please scroll down to see the full text article.

2008 J. Phys.: Condens. Matter 20 335104

(<http://iopscience.iop.org/0953-8984/20/33/335104>)

View [the table of contents for this issue](#), or go to the [journal homepage](#) for more

Download details:

IP Address: 129.252.86.83

The article was downloaded on 29/05/2010 at 13:54

Please note that [terms and conditions apply](#).

Dielectric relaxation study of the dynamics of monosaccharides: D-ribose and 2-deoxy-D-ribose

K Kaminski¹, E Kaminska¹, P Włodarczyk¹, M Paluch¹, J Ziolo¹
and K L Ngai²

¹ Institute of Physics, Silesian University, ulica Uniwersytecka 4, 40-007 Katowice, Poland

² Naval Research Laboratory, Washington, DC 20375-5320, USA

Received 8 May 2008, in final form 23 June 2008

Published 22 July 2008

Online at stacks.iop.org/JPhysCM/20/335104

Abstract

The dielectric loss spectra of two closely related monosaccharides, D-ribose and 2-deoxy-D-ribose, measured at ambient and elevated pressures are presented. 2-deoxy-D-ribose and D-ribose are respectively the building blocks of the backbone chains in the nucleic acids DNA (deoxyribonucleic acid) and RNA (ribonucleic acid). Small differences in the structure between D-ribose and 2-deoxy-D-ribose result in changes of the glass transition temperature T_g , as well as the dielectric strength and activation enthalpy of the secondary relaxations. However, the frequency dispersion of the structural α -relaxation for the same relaxation time remains practically the same. Two secondary relaxations are present in both sugars. The slower secondary relaxation shifts to lower frequencies with increasing applied pressure, but not the faster one. This pressure dependence indicates that the slower secondary relaxation is the important and 'universal' Johari–Goldstein β -relaxation of both sugars according to one of the criteria set up to classify secondary relaxations. Additional confirmation of this conclusion comes from good agreement of the observed relaxation time of the slower secondary relaxation with the primitive relaxation time calculated from the coupling model. All the dynamic properties of D-ribose and 2-deoxy-D-ribose are similar to the other monosaccharides, glucose, fructose, galactose and sorbose, except for the much larger relaxation strength of the α -relaxation of the former compared to the latter. The difference may distinguish the chemical and biological functions of D-ribose and 2-deoxy-D-ribose from the other monosaccharides.

(Some figures in this article are in colour only in the electronic version)

1. Introduction

D-ribose ($C_5H_{10}O_5$), sometimes referred to as just ribose, is a monosaccharide containing five carbon atoms forming a six-membered ring (pyranose) composed of five carbon atoms and one oxygen. Conventionally structures of the D-ribose and other pentoses were presented as furanoses. However, current investigation with use of x-ray spectroscopy indicated that both D-ribose and other pentoses form pyranose rings in crystal. Hydroxyl groups are attached to three of the carbons. The other carbon and a hydroxyl group are attached to one of the carbon atoms adjacent to the oxygen. Closely related to D-ribose is 2-deoxy-D-ribose ($C_5H_{10}O_4$). The main difference between the two compounds is that, in the case of 2-deoxy-D-ribose, the hydroxyl group attached to the carbon (#2) is reduced to hydrogen (see figure 1).

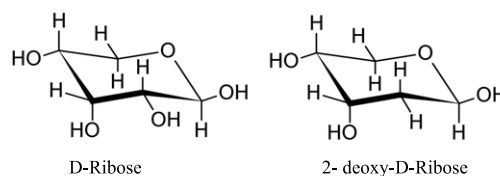


Figure 1. The chemical structures of D-ribose and 2-deoxy-D-ribose.

2-deoxy-D-ribose and D-ribose are respectively the building blocks of the backbone chains in the nucleic acids DNA (deoxyribonucleic acid) and RNA (ribonucleic acid). The presence of 2-deoxy-D-ribose instead of D-ribose is one of the differences between DNA and RNA. The derivatives of D-ribose and 2-deoxy-D-ribose play important roles in biology

as well as applications as sugars in pharmaceuticals and food science like the other monosaccharides, glucose, fructose, galactose and sorbose.

The molecular relaxation dynamics of these sugars are of fundamental interest in the glass transition and are useful to know for applications in food science and the pharmaceutical industry. Experimental investigations toward this goal have been made on various sugars and their mixtures with water [1–9] principally by dielectric relaxation and enthalpy relaxation [10]. Dielectric spectra of the monosugars reveal two clearly resolved relaxation peaks. The slower one is the α -relaxation responsible for the liquid–glass transition and the much faster one is the secondary relaxation (called γ -relaxation in the present study). Pressure insensitivity of the secondary γ -relaxation to applied pressure indicates that it is of intramolecular origin [11]. However, explanation of the molecular mechanism of this process is still a controversial issue. One can cite a few possibilities suggested in the literature including rotation of the hydroxyl groups, motion within the sugar ring, hydrogen bonds and boat–chair interconversion. In our recent study of the sugars by broadband dielectric spectroscopy, the relaxation mechanisms of D-ribose, as well as glucose, galactose, sorbose and fructose, were characterized [12]. In these systems we found the presence of a new secondary relaxation process appearing as an excess wing on the high frequency side of the α -relaxation in the dielectric loss spectra. Our studies augmented by the application of pressure showed that this process is sensitive to pressure and hence a true Johari–Goldstein (JG) secondary β -relaxation [12]. Recent advances in research of the relaxation dynamics in glass-forming substances have shown that the JG secondary β -relaxation is ubiquitous, bears a strong connection with the structural α -relaxation and hence plays a fundamental role in the glass transition [11, 13–16]. Therefore it would be interesting to inquire whether the JG secondary β -relaxation is present in 2-deoxy-D-ribose or not. This is one of the purposes of this paper. The other one is to get more insight into the molecular mechanism responsible for the γ -relaxation in D-ribose and 2-deoxy-D-ribose and in the entire family of the sugars.

2. Experimental details

Isobaric dielectric measurements on 2-deoxy-D-ribose at ambient pressure were carried out using a Novo-Control GMBH Alpha dielectric spectrometer (10^{-2} – 10^7 Hz) and Agilent E 4991 A impedance analyzer (10^6 – 10^9 Hz). The temperature was controlled by the Quattro system, employing a nitrogen-gas cryostat, and temperature stability of the sample was achieved to better than 0.1 K. The anhydrous 2-deoxy-D-ribose and D-ribose samples of over 98% purity were purchased from Aldrich Chemicals. Since we were aware of the possibility of caramelization of these compounds at high temperatures, melting of both D-ribose and 2-deoxy-D-ribose was carried out with care. Fortunately, the temperature of caramelization of both saccharides is much higher than their melting temperature and caramelization was avoided.

The other problem which has to be avoided in dielectric measurements of the saccharides is the presence of water in the samples. D-ribose and 2-deoxy-D-ribose have a number of hydroxyl groups, making them highly hygroscopic. The presence of water has a large effect on the molecular mobility of hydrophilic glass-formers. One indication of the presence of water is the change of the glass transition temperature T_g . It is commonly found that even small traces of water change significantly the T_g of the saccharides. Recently we have performed dielectric relaxation measurements on glucose, fructose, galactose, sorbose [12] and sucrose [17] and the values of the glass transition temperatures of these sugars obtained from dielectric relaxation data are in nearly perfect agreement with that determined from differential scanning calorimetry DSC for anhydrous samples. The present dielectric measurements of 2-deoxy-D-ribose and D-ribose were performed in the same way as was done in the case of the six other carbon monosaccharides. Thus, despite the lack of any literature data about values of T_g for both systems studied herein, we can assume that there is no water present in 2-deoxy-D-ribose and D-ribose.

Isobaric measurements were performed starting at temperatures way above the glass transition temperature T_g , to temperatures deep in the glassy state. Isothermal dielectric relaxation measurements on D-ribose at elevated pressures were made before and the experimental set-up for high pressure measurements was described in detail in reference [18].

3. Results and discussions

The dielectric loss data of D-ribose (upper panel) and 2-deoxy-D-ribose (lower panel) are shown in figure 2. The loss spectra of both compounds reveal two clearly resolved relaxation peaks contributed by the α -relaxation and a secondary relaxation. However, when temperature is lowered sufficiently below T_g and the α -loss peak is moved out of the experimental frequency window, a shoulder appears in the loss spectra. This new feature indicates the presence of another secondary relaxation (labeled β in figure 2) located at frequencies intermediate between the α -relaxation and the resolved faster secondary relaxation (labeled γ). The same evidence for β -relaxation is present in the other sugars studied including fructose, galactose, glucose and sorbose [12]. In galactose and sorbose, when the temperature is decreased sufficiently below T_g , the shoulder is transformed to a loss peak which provides unequivocal evidence of the presence of the β -relaxation in the sugars. The shoulder found in D-ribose has been made more evident by applying pressure to show the β -relaxation is indeed present. Another benefit of obtaining dielectric relaxation data of D-ribose and fructose under applied pressure is the demonstration of the shift of the β -relaxation loss peak to lower frequencies in concert with the α -relaxation. On the other hand, the γ -relaxation does not shift with pressure. The difference in pressure dependence distinguishes the β -relaxation from the γ -relaxation in that the β -relaxation is correlated with the α -relaxation. This is one of several correlations that a special class of secondary relaxations (called the Johari–Goldstein β -relaxation [11] to honor the

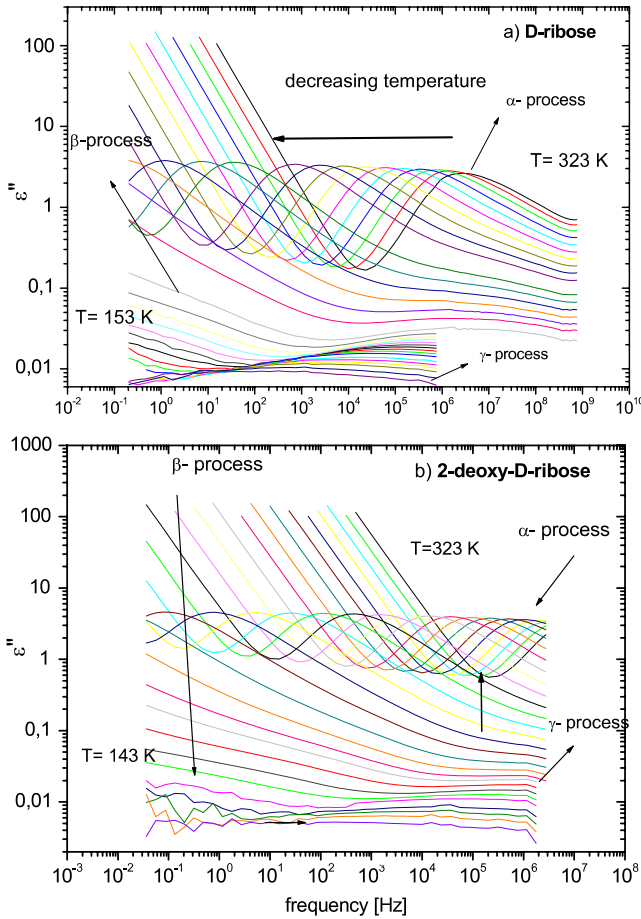


Figure 2. Dielectric spectra of D-ribose (a) and 2-deoxy-D-ribose (b) measured at ambient pressure ($P = 0.1$ MPa) and different temperatures (from 50°C down to -120°C , and from 50°C down to -130°C , respectively).

researchers who found the presence of secondary relaxation in totally rigid glass-formers without an intramolecular degree of freedom [16]) has with the α -relaxation. The use of pressure sensitivity to distinguish different kinds of relaxation processes was made also in conducting polymer networks to distinguish interchain from intrachain electric charge flow mechanisms [19]. Additional experimental evidence that the Johari–Goldstein β -relaxation and the α -relaxation are not independent processes comes from nuclear magnetic resonance (NMR) experiments [20] which showed that the α -relaxation was modified by suppressing some part of the β -relaxation. All these experimental evidences show the fundamental importance of the Johari–Goldstein β -relaxation in the glass transition. Hence, an important aspect of our work is finding the Johari–Goldstein β -relaxation also in D-ribose and 2-deoxy-D-ribose.

The faster γ -relaxation, although clearly resolved in the dielectric loss spectra of the D-ribose and 2-deoxy-D-ribose, has no pressure dependence. This is indicative that it originates from some local intramolecular degree of freedom. It is a characteristic feature in the dynamics of the whole family of the monosaccharides with comparable relaxation times and activation energies in their glassy states. The general properties

of this γ -relaxation process are (i) large dielectric strength, (ii) activation energy E_a lies within the range from 42 to 62 kJ mol^{-1} [21], (iii) the dielectric strength of this process decreases much more rapidly with decreasing temperature than that of secondary relaxations in most other glass-forming liquids and (iv) its dielectric strength increases with increase in the molecular weight of the sugars. The origin of this process was the subject of many investigations, both theoretical [22] and experimental [1–9]. However, there is still no consensus on what exactly is the molecular motion responsible for the γ -relaxation.

From figure 2 one can see that the dielectric strength of the γ -relaxation of the 2-deoxy-D-ribose is smaller than that of the D-ribose. Such a situation was also observed when comparing the γ -relaxation of the six carbon saccharides D-mannose and L-rhamnose. L-rhamnose is a reduced sugar having a similar structure to D-mannose but the carbon C(#6) has only one methyl group attached to it, while in D-mannose there is the hydroxy methyl group linked to this carbon [21]. Such a difference in the dielectric relaxation strength of the γ -relaxation in two closely related sugars indicates that hydroxyl groups attached to the sugar ring may be responsible for the γ -relaxation observed in the dielectric loss spectra. This local origin of the γ -relaxation in the monosaccharides naturally explains why it is insensitive to applied pressure, as found by experiments performed on D-ribose and D-fructose [12]. Thus the experimental facts described here support a connection between the γ -relaxation and the intramolecular motion of the hydroxyl groups attached to the sugar ring.

In figure 3 the loss spectra of 2-deoxy-D-ribose and D-ribose obtained at ambient pressure are compared. The two spectra are chosen to have the same loss peak frequency of about 1 Hz. The main part of the α -loss peaks of 2-deoxy-D-ribose and D-ribose are practically identical. This is not surprising in view of the same ring structure and the same number of carbon atoms, resulting in little or no change in the intermolecular interaction and hence nearly the same frequency dispersion of the α -relaxation. Additionally, in panels (b) and (c) of figure 3 we present superimposed loss spectra measured at different temperatures of D-ribose and 2-deoxy-D-ribose, respectively. One can see that the shapes of the α -relaxation peaks of both sugars are the same over the temperature ranges indicated. In fact, the frequency dispersion of the α -loss peak is the same at all the chosen temperatures.

The main parts of the loss spectra of both sugars are well fitted by the one-sided Fourier transform of the Kohlrausch–Williams–Watts (KWW) function [23, 24]:

$$\phi(t) = \exp[-(t/\tau_\alpha)^{1-n}] \quad (1)$$

with $(1 - n) = 0.55$. The intense resolved γ -relaxation accounts mainly for the excess of the data over the KWW fit. The Johari–Goldstein (JG) β -relaxation found below T_g certainly continues to show up above T_g . Although it gives some contribution to the loss spectrum, the contribution is not significant because of its small dielectric strength. Therefore, we fit the isothermal loss spectra of the D-ribose and 2-deoxy-D-ribose at temperatures above T_g by a superposition of the

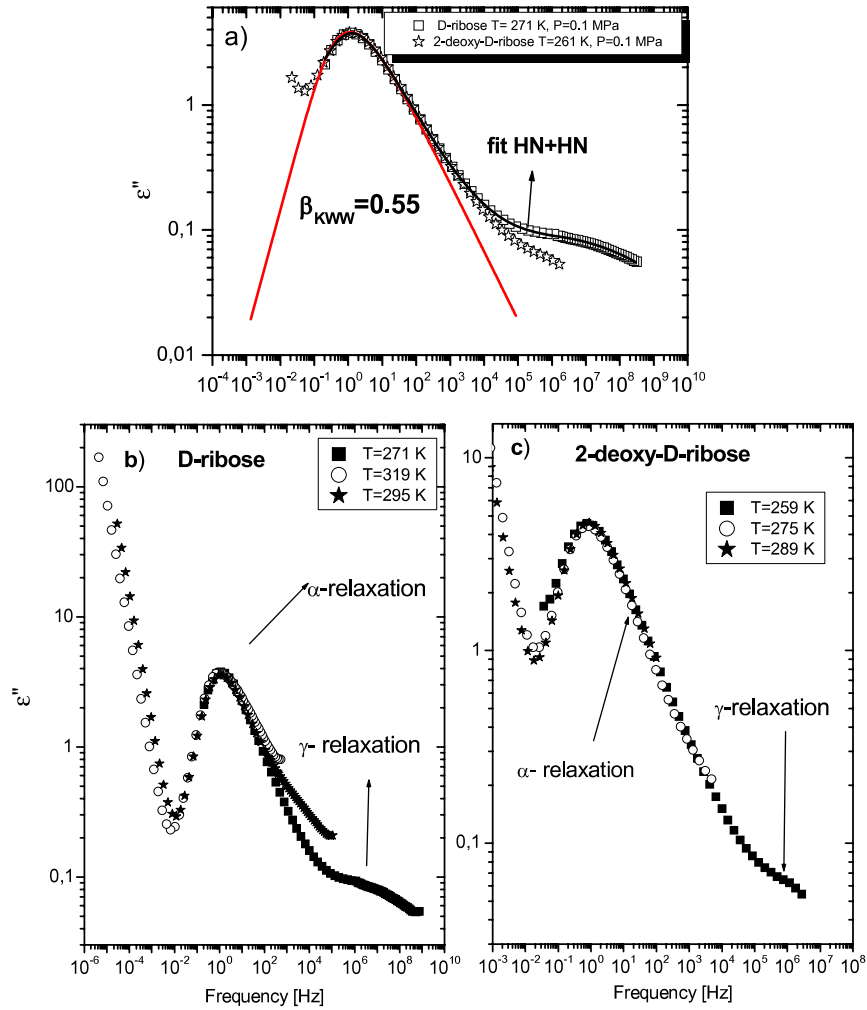


Figure 3. Comparison of the loss spectra obtained from isobaric measurements for 2-deoxy-D-ribose and D-ribose. The solid red curve is a Kohlrausch–Williams–Watts function with $n \equiv (1 - \beta) = 0.45$ (panel (a)). The solid black line represents the sum of two HN fits to the D-ribose loss spectrum measured at $T = 271$ K. In panel (b) are presented superimposed loss spectra of the D-ribose measured at $T = 271$ K (filled squares), 295 K (filled stars) and 319 K (open circles). The loss spectra obtained at $T = 295$ and 319 K were shifted horizontally to superimpose with those collected at $T = 271$ K. In panel (c) superimposed loss spectra of the 2-deoxy-D-ribose measured at $T = 259$ K (filled squares), 275 K (open circles) and 289 K (filled stars) are shown. The loss spectra were superposed on those obtained at $T = 259$ K.

Havriliak–Negami functions for the α -relaxation and for the γ -relaxation times:

$$\varepsilon''(\omega) = \sum_i \text{Im} \left(\frac{\Delta \varepsilon_i}{(1 + (i\omega\tau_i)^{\alpha_i})^{\beta_i}} \right) \quad (2)$$

In equation (2), $i = 1$ and 2 stand for the α -relaxation and the γ -relaxation, respectively. Usually in fitting secondary relaxation one use the symmetric Cole–Cole function. However, in the case of saccharides the Cole–Cole function does not describe well the γ -relaxation, because of its asymmetric shape. From the fits, the α - and γ -relaxation times, τ_α and τ_γ of 2-deoxy-D-ribose and D-ribose were determined and plotted against reciprocal temperature in figure 4. The dependences of the α -relaxation times on temperature were well described by the Vogel–Fulcher–

Tammann–Hesse equation:

$$\tau_\alpha = \tau_{\text{VFT}} \exp \left(\frac{D_T}{T - T_0} \right). \quad (3)$$

The temperature dependences of the γ -relaxation times were fitted to the Arrhenius equation:

$$\tau_\gamma = \tau_\infty \exp(E_a/RT). \quad (4)$$

Parameters used in the fit are given in table 1. From the VFTH fits, the glass transition temperatures T_g of D-ribose and 2-deoxy-D-ribose were determined to be 259 K and 249 K, respectively. Here the T_g is defined as the temperature at which the dielectric relaxation time τ_α is equal to 100 s, a commonly used procedure of obtaining T_g from dielectric data. One can see that the 10 K difference in glass transition temperature of the two related sugars is not small. This difference is understandable because carbon (#2) in D-ribose has one –OH group and one H, while carbon (#2) in 2-deoxy-D-ribose

Table 1. Fitting parameters of the VFTH and Arrhenius equations.

	VFTH parameters			Arrhenius parameters			
	Log τ_{VFTH}	D_T	T_0 (K)	Log τ_∞	E_a (kJ mol ⁻¹)	Fragility, m	T_g (K)
D-ribose	-15.60 ± 0.1	2323 ± 37	202 ± 1	-14.18 ± 0.05	33.50 ± 0.20	79 ± 3	259
2-deoxy-D-ribose	-14.72 ± 0.2	2209 ± 49	192 ± 1	-15.08 ± 0.25	34.50 ± 0.9	73 ± 3	249

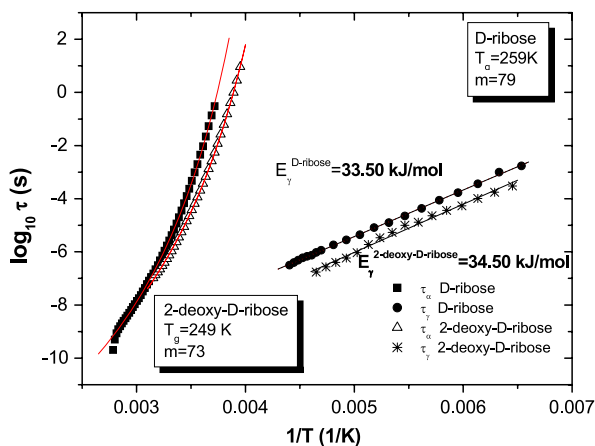


Figure 4. Temperature dependences of the structural (α) and the secondary γ -relaxation times of D-ribose and 2-deoxy-D-ribose. The black solid lines are the fits to the secondary γ -relaxations using the Arrhenius law. The red lines represent the VFTH behavior.

instead has two H. Thus the hydrogen bonding of the extra –OH group in D-ribose may cause the increase of T_g above that of 2-deoxy-D-ribose. In the case of six-carbon sugars L-rhamnose and D-mannose having $T_g = 310$ K and 311 K [21], respectively, this difference of 1 K is much less. This disparity in the change of the glass transition temperature in the two systems can be explained. D-mannose and L-rhamnose have hydroxyl groups attached to the sugar ring in different axial and equatorial positions, while in the case of D-ribose and 2-deoxy-D-ribose the positions of the hydroxyl group are the same. Thus the effect of a significant change in T_g in the case of D-ribose and 2-deoxy-D-ribose is caused principally by the lack of the one hydroxyl group at carbon (#2) in 2-deoxy-D-ribose compared with D-ribose.

From the VFTH fits to the temperature dependences of the τ_α of the two sugars their ‘fragilities’ or steepness indices m , defined by [25]:

$$m = d \log_{10} \tau_\alpha / d(T_g/T) |_{(T_g/T)=1} \quad (5)$$

were calculated. Their values are 79 and 73 for D-ribose and 2-deoxy-D-ribose, respectively. One can classify both systems as moderately fragile glass-forming liquids. The difference in fragility between the two monosaccharides is small, although the slightly larger fragility of D-ribose than 2-deoxy-D-ribose may have something to do with the fact that D-ribose has an extra hydroxyl group and hence an enhanced ability to form hydrogen bonds. The same observation was made by Döb *et al* [26] in the series of polyalcohols where the fragility index increases with increasing number of hydroxyl groups per molecule in the order of glycerol, threitol, xylitol and sorbitol.

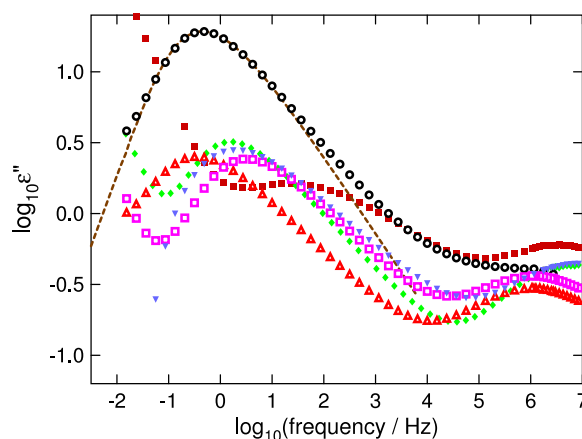


Figure 5. Comparison of D-ribose with other sugars: D-ribose (open black circles fitted by the one-sided Fourier transform of the Kohlrausch function with $n = 0.45$ shown as the dashed line), fructose (open orange triangles), sorbose (open magenta squares), glucose (closed green diamonds) and galactose (blue closed inverted triangles).

The values of the activation energies E_a for the γ -relaxation of the D-ribose and 2-deoxy-D-ribose are 33.50 kJ mol⁻¹ and 34.50 kJ mol⁻¹, respectively. Earlier in this paper it was mentioned that activation energies of the γ -relaxation observed in typical monosaccharides with six carbon atoms lie within the range from 42 to 62 kJ mol⁻¹, including also disaccharides and polysaccharides. Obviously the values of activation energies of the γ -relaxation of the 2-deoxy-D-ribose and D-ribose are lower than 42 kJ mol⁻¹. One of the probable explanations of this peculiarity may be the fact that both D-ribose and 2-deoxy-D-ribose have one carbon, and thus one hydroxyl group, less than the other monosaccharides such as glucose, fructose, galactose and mannose. It also implies that dielectric strengths of the γ -relaxations of D-ribose and 2-deoxy-D-ribose, relative to that of the α -relaxation, are much smaller than that observed in fructose, sorbose, glucose, galactose or other six-carbon monosaccharides. This is demonstrated in figure 5.

Another interesting observation is that the activation energy of the γ -relaxation of 2-deoxy-D-ribose is a little bit larger than that of D-ribose. Although this difference is very small it is quite surprising, because one could expect a completely different scenario. D-ribose has one extra hydroxyl group more than 2-deoxy-D-ribose, implying greater affinity of the former to form hydrogen bonds and hence larger γ -relaxation activation energy than the latter. This peculiar situation indicates that the origin of the γ -relaxation is not trivial. From one aspect of the experimental evidence we have

shown that there is some relationship between the hydroxyl groups and the origin of the γ -relaxation of both D-ribose and 2-deoxy-D-ribose. However, the comparison of the activation energies of the γ -relaxations of D-ribose and 2-deoxy-D-ribose showed that such a simple explanation of γ -relaxations from local hydroxyl groups may not hold. The activation energies of the hydroxyl group motions or rotations are all within the range of a few kJ mol^{-1} or even less, and thus cannot account for the much lower activation energies (33.50 and $34.50 \text{ kJ mol}^{-1}$) of D-ribose and 2-deoxy-D-ribose than those of the other six-carbon monosaccharides. This conundrum may be caused by additional contributions to the γ -relaxation from intermolecular interaction, as was pointed out by Faivre [9], or some conformational changes of the sugar ring.

Although the γ -relaxation has larger dielectric strength due to involvement of the hydroxyl groups, the JG β -relaxation plays a fundamental role in the glass transition [11, 13, 20, 27] and it will be the focus of further discussion. All the isothermal loss $\varepsilon''(\nu)$ were measured above $\nu_{\min} = 3.6 \times 10^{-2} \text{ Hz}$. This limitation of the frequency range of measurement to above ν_{\min} makes it impossible to show the presence of both the α - and the JG β -relaxation in the dielectric spectrum taken at the same temperature. Nevertheless, there is a procedure to do this with a good approximation if the frequency dispersion of the α -loss peak does not change with decreasing temperature near and above T_g . This condition is satisfied in D-ribose and 2-deoxy-D-ribose. As shown in figure 3, the α -relaxation loss peak of D-ribose and 2-deoxy-D-ribose shows no change in shape and intensity over some ranges of temperatures near and above T_g . Hence, we can expect that this trend will continue down to a lower temperature T_{s0} , where the shoulder of $\varepsilon''(\nu)$ indicates the presence of the JG β -relaxation. For 2-deoxy-D-ribose in figure 6, we have chosen the loss data at $T_{s0} = 243 \text{ K}$. With this assumption, we horizontally shift the measured $\varepsilon''(\nu)$ at T_{s1} , the next higher measurement temperature than T_{s0} , to overlap the actually measured values of $\varepsilon''(\nu)$ at T_{s0} near ν_{\min} . Only the $\varepsilon''(\nu)$ data at T_{s1} near and above $\varepsilon''(\nu_{\min})$ at T_{s0} are retained. In this way, we have extended the supposedly $\varepsilon''(\nu)$ data at T_{s0} to frequencies down to $\log(\nu_{\min}) - \log(\Delta\nu_1)$, where $\log(\Delta\nu_1)$ is the magnitude of the horizontal shift. The extensions of $\varepsilon''(\nu)$ to lower frequencies by this procedure are not large, and hence they are approximately the $\varepsilon''(\nu)$ data at T_{s0} , had measurements been possible at frequencies down to $\log(\nu_{\min}) - \log(\Delta\nu_1)$. The same procedure is repeated for the data taken at T_{s2} , the next higher measurement temperature than T_{s1} , and so on and so forth for multiple times until the α -loss peak evident at T_{sf} has been captured in the supposedly isothermal $\varepsilon''(\nu)$ spectrum of 2-deoxy-D-ribose at $T_{s0} = 243 \text{ K}$ by the master curve shown in figure 6. The filled black squares on the master curve are the actually measured $\varepsilon''(\nu)$ at $T_{s0} = 243 \text{ K}$ and the ‘data’ at frequencies below ν_{\min} are the extensions constructed from the measured isothermal $\varepsilon''(\nu)$ data at higher temperatures also shown in the same figure (where the invariance of the shape of the α -loss peak with temperature can also be seen). The α -loss peak frequency ν_α of the master curve is $3.5 \times 10^{-5} \text{ Hz}$. The dashed line is the KWW fit of the α -loss peak with $n = 0.45$, and the deviations of the data from the fit on the high frequency flank is due to the contribution from the submerged

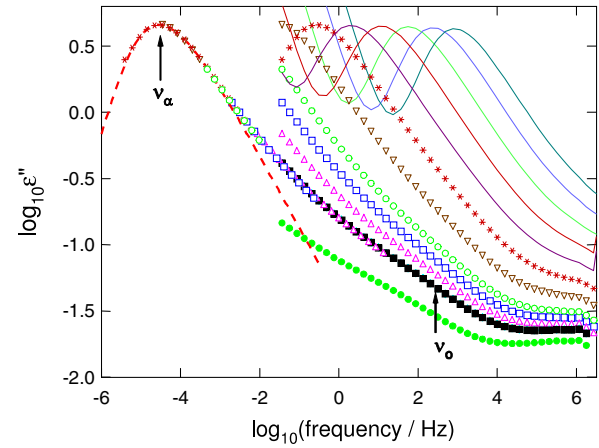


Figure 6. Construction of an approximate isothermal loss spectrum of 2-deoxy-D-ribose complete with the α -loss peak and the JG β -relaxation (indicated by the inflection) at $T = 243 \text{ K}$ by successfully shifting the data at higher temperatures in a procedure described in the text. The data used to construct the spectrum are shown by symbols. Higher temperature data not used are shown by lines.

JG β -relaxation, which shows up only as a broad shoulder in the spectrum. The location of the shoulder over the broad range from 1 to 10^4 Hz is reminiscent of the broad frequency dispersion of the JG β -relaxation in the glassy state found in many other glass-formers. One way to obtain an estimate of its characteristic relaxation time τ_β is to calculate the primitive relaxation time τ_0 of the coupling model [11, 13, 27–30]:

$$\tau_0 = (t_c)^n (\tau_\alpha)^{1-n}. \quad (6)$$

Here $(1 - n)$ and τ_α are respectively the stretch exponent and the relaxation time of the Kohlrausch function in equation (1), the one-sided Fourier transform of which fits the shape of the α -loss peak, and t_c is 2 ps. The primitive relaxation of the coupling model (CM) is a local relaxation involving the entire molecule and has properties mimicking that of the α -relaxation, including the shift of relaxation time with applied pressure as found for the JG β -relaxation of D-ribose and other six-carbon monosaccharides. Therefore the approximate relation:

$$\tau_0 \approx \tau_\beta \quad (7)$$

is expected as verified repeatedly by experiment in many glass-formers [11, 13, 28–30]. On combining equations (6) and (7) and expressing the result in terms of the relaxation frequencies $\nu_\alpha \equiv (1/2\pi\tau_\alpha)$ and $\nu_\beta \equiv (1/2\pi\tau_\beta)$, we have the following formula to calculate ν_{JG} :

$$\log \nu_\beta \approx \log \nu_0 = (1 - n) \log \nu_\alpha + 10.9n \quad (8)$$

where the units of ν_{JG} and ν_α are in Hz. The value of ν_0 calculated by equation (8) from the known values of $n = 0.45$ and $\nu_\alpha = 3.5 \times 10^{-5} \text{ Hz}$ is indicated by the location of the vertical arrow in figure 6. The location of ν_0 is near the point of inflection of the loss data, which is a good indication where ν_β is supposed to be.

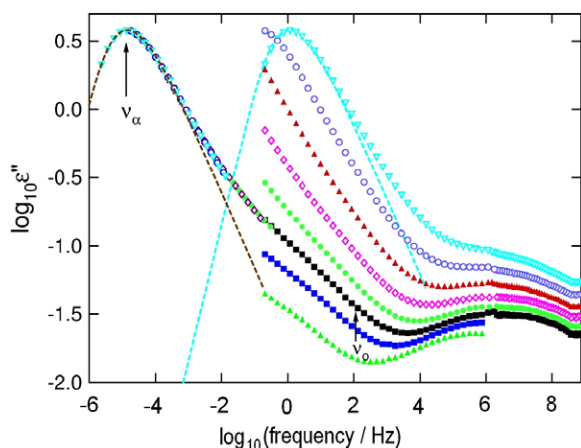


Figure 7. Construction of an approximate isothermal loss spectrum of D-ribose at ambient pressure complete with the α -loss peak and the JG β -relaxation (indicated by the inflection) at $T = 251$ K by successfully shifting the data at higher temperatures in a procedure as described in the text.

The same operation on the isothermal data of 2-deoxy-D-ribose in figure 6 was performed on the isothermal dielectric data of D-ribose at ambient pressure and at an elevated pressure of 5000 bar or 500 MPa. The resulting master loss curves are shown in figure 7 for ambient pressure and figure 8 for 5000 bar. The frequency dependence of the α -loss peak near T_g of D-ribose at ambient pressure and at 5000 bar are the same and are well fitted to the one-sided Fourier transform of the Kohlrausch function with $n = 0.45$. Together with $\nu_\alpha = 1.3 \times 10^{-5}$ Hz and $\nu_\alpha = 5.3 \times 10^{-6}$ Hz for the master curves of D-ribose at ambient pressure and 5000 bar respectively, the corresponding values of ν_0 are calculated by equation (8). The location of ν_0 for each case is indicated by the vertical arrow in figures 7 and 8. A particularly clear inflection is shown by the loss data of D-ribose at 5000 bar, which is the best evidence of the presence of the JG relaxation. The inflection occurs at frequencies near the calculated ν_0 , which supports the relation given by equations (6) and (7) of the CM. Included in figure 8 for comparison with isothermal loss spectra taken at 5000 bar are two ambient pressure spectra at $T = 267$ and 269 K. The frequency dispersions of the spectra at 5000 bar and at 1 bar are nearly identical. Thus, this D-ribose offers another example of the invariance of the frequency dispersion of the α -dispersion measured at different combinations of pressure and temperature but having the same relaxation time [31, 32]. Hydrogen-bonded polyalcohols such as glycerol and sorbitol [33] as well as m-fluoroaniline [34] are exceptions to this rule, showing broadening of the α -dispersion with applied pressure because of the breakage of hydrogen bonds at higher temperature accompanied with elevated pressure used to maintain the same relaxation time. It is unclear at this time why the hydrogen-bonded D-ribose does not behave in the same way.

Finally, we further shift horizontally the master curves of 2-deoxy-D-ribose and D-ribose in figures 6 and 7 at ambient pressure to have the maxima of the loss peaks at the same frequency, $\nu_\alpha = 5.3 \times 10^{-6}$ Hz, as the master curve of D-ribose under 5000 bar in figure 8. Vertical shifts are made to

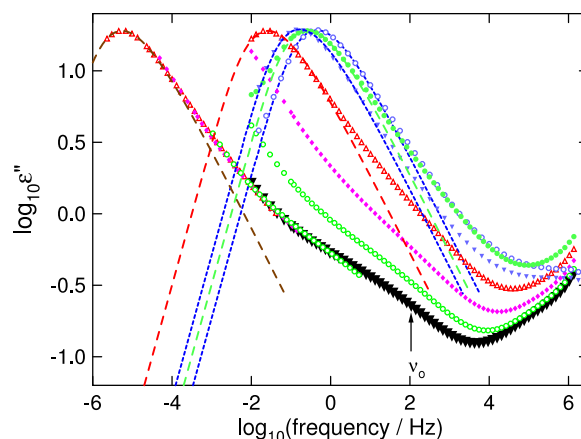


Figure 8. Construction of an approximate isothermal loss spectrum of D-ribose at elevated pressure of 5000 bar complete with the α -loss peak and the JG β -relaxation (indicated by the inflection) at 278.2 K by successfully shifting the data at higher temperatures in a procedure as described in the text. The blue open circles and closed inverted triangles are spectra of D-ribose taken under ambient pressure. All dashed lines are KWW fits to the spectra with $n = 0.45$.

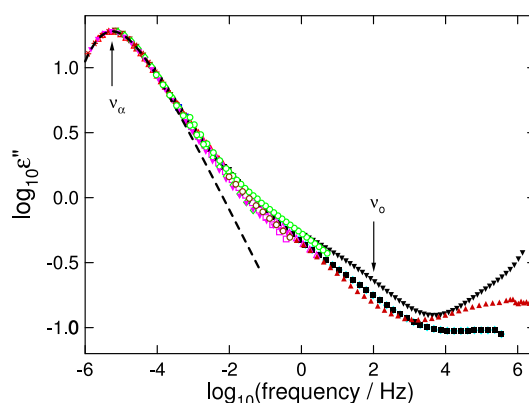


Figure 9. Comparing the master curves of 2-deoxy-D-ribose and D-ribose at ambient pressure, and D-ribose at elevated pressure of 5000 bar at the same ν_α , to show nearly identical features including the same Kohlrausch function fit of the α -loss peak and approximately the same location of the JG β -relaxation. D-ribose at 5000 bar uppermost (inverted triangles), 2-deoxy-D-ribose (black closed squares) and D-ribose at 1 bar (red closed triangles).

have the same maximum loss for all at $\nu_\alpha = 5.3 \times 10^{-6}$ Hz. From the result shown in figure 9, it can be seen that, in all three cases, the frequency dispersion of the α -relaxation is the same and has the same n for the Kohlrausch function fits. Also, the inflections of the loss data in all three sets of data occur approximately within the same frequency range, indicating the same location of ν_β for all three cases. The location of ν_β indicated by the inflection is consistent with the calculated primitive relaxation frequency ν_0 of the CM by equation (8).

Let us return to figure 5 where the dielectric loss data of D-ribose are compared with those of the other monosaccharides, fructose, galactose, sorbose and glucose, all with peak frequencies in the neighborhood of 1 Hz and at ambient pressure. The purpose of this comparison is to show that the α -loss peak of D-ribose (and also 2-deoxy-D-ribose) is much

more prominent than the other sugars. Relative to the γ -loss peak, the maximum of the α -loss peak of D-ribose is about one order of magnitude larger than that of the other sugars. For this reason, significant excess of the loss data over that Kohlrausch fit on the high frequency flank of the α -loss peak (i.e. the presence of a prominent excess wing) can be seen from the spectra of D-ribose in figure 5, indicating the presence of the unresolved JG β -relaxation at lower frequencies than the resolved γ -relaxation. On the other hand, for the other sugars, the much reduced α -loss is merged with the contribution to the loss from the JG β -relaxation, resulting in no excess wing being observed that can be attributed to the contribution of the unresolved JG β -relaxation. The effect is a broadening of the α -loss peak of fructose, glucose, galactose and sorbose in their liquidus states. Any attempt to fit the loss spectra by the Kohlrausch function will give a larger value of n than the actual value of the coupling parameter in equations (6) and (8). Thus, unlike D-ribose and 2-deoxy-D-ribose, there is no reliable way to obtain the actual value of n to calculate the primitive relaxation time of the coupling model [11, 13] and compare it with the experimental JG β -relaxation time for fructose, glucose, galactose and sorbose.

4. Conclusions

Except for a slight decrease in the glass transition temperature, the relaxation dynamics of 2-deoxy-D-ribose are similar in every respect to D-ribose. They have identical frequency dispersion of the α -relaxation and the same stretching exponent of the Kohlrausch function that fits it. Two secondary relaxations are present in both sugars. The slower β -relaxation is pressure-dependent while the faster γ -relaxation is not. There is also approximate correspondence between the primitive relaxation time of the coupling model with the β -relaxation time deduced from the location of an inflection found in the loss spectrum. These properties of the β -relaxation in D-ribose and 2-deoxy-D-ribose indicate that they belong to the important class of secondary relaxations called the Johari–Goldstein β -relaxations that bear a fundamental relation to the α -relaxation and hence play an important role in the glass transition. On the other hand, the faster γ -relaxation is insensitive to applied pressure and has other properties indicating its intramolecular origin. Its large dielectric strength suggests that it involves the hydroxyl units. The relaxation time of the γ -relaxation of 2-deoxy-D-ribose is slightly shorter and its activation energy a bit higher than the corresponding quantities of D-ribose. The γ -relaxation times of D-ribose and 2-deoxy-D-ribose are much shorter and activation energies noticeably smaller than those of the other monosaccharides. The relaxation strength of the α -relaxation of D-ribose and 2-deoxy-D-ribose is about one order of magnitude larger than that of the other monosaccharides including fructose, glucose, galactose and sorbose. These differences may come from D-ribose and 2-deoxy-D-ribose having five carbons in the ring compared with six carbons in the other monosaccharides.

Acknowledgments

Financial support of the Committee for Scientific Research, Poland KBN, grant no. N N202 007534 is gratefully

acknowledged. This work at the Naval Research Laboratory was supported by the Office of Naval Research. KK acknowledges financial assistance from FNP (2008). J Ziolo wishes to acknowledge the financial support of the Committee for Scientific Research, Poland (KBN, grant no. N202 147 32/4240).

References

- [1] Chan R, Pathmanathan K and Johari G P 1986 *J. Phys. Chem.* **90** 6358
- [2] Noel T R, Ring S G and Whittam M A 1976 *J. Phys. Chem.* **96** 5667
- [3] Tombari E, Cardellia C, Salvettia G and Johari G P 2001 *J. Mol. Struct.* **559** 245
- [4] Gangasharan and Murthy S S N 1993 *J. Chem. Phys.* **99** 9865
- [5] Tyagi M and Murthy S S N 2006 *Carbohydr. Res.* **341** 650
- [6] Jeong-Ah S, Jiyoung O, Hyun-Joung K, Hyung Kook K and Yoon-Hwae H 2006 *AIP Conf. Proc.* **832** 37
- [7] Noel T R, Parker R and Ring S G 1996 *Carbohydr. Res.* **282** 193
- [8] Champion D, Maglione M, Niquet G, Simatos D and Le Meste M 2003 *J. Therm. Anal. Calor.* **71** 249
- [9] Faivre A, Niquet G, Maglione M, Fornazero J, Jal J F and David L 1999 *Eur. Phys. J. B* **10** 277
- [10] Wungtanagorn R and Schmidt S J 2001 *Thermochim. Acta* **369** 95
- [11] Ngai K L and Paluch M 2004 *J. Chem. Phys.* **120** 857
- [12] Kaminski K, Kaminska E, Paluch M, Ziolo J and Ngai K L 2006 *J. Phys. Chem. B* **110** 25045
- [13] Ngai K L 2003 *J. Phys.: Condens. Matter* **15** S1107
- [14] Paluch M, Roland C M, Pawlus S, Ziolo J and Ngai K L 2003 *Phys. Rev. Lett.* **91** 115701
- [15] Hensel-Bielowka S, Paluch M and Ngai K L 2005 *J. Chem. Phys.* **123** 014502
- [16] Johari G P and Goldstein M 1970 *J. Chem. Phys.* **53** 2372
- [17] Kaminski K, Kaminska E, Hensel-Bielowka S, Chelmecka E, Paluch M, Ziolo J, Wlodarczyk P and Ngai K L 2008 *J. Phys. Chem. B* **112** 7662
- [18] Urbanowicz P, Rzoska S J, Paluch M, Sawicki B, Szulc A and Ziolo J 1995 *J. Chem. Phys.* **201** 575
- [19] Papathanassiou A N, Sakellis I and Grammatikakis J 2006 *Appl. Phys. Lett.* **89** 222905
- [20] Papathanassiou A N, Sakellis I and Grammatikakis J 2007 *Appl. Phys. Lett.* **91** 202103
- [21] Böhmer R, Diezemann G, Geil B, Hinze G, Nowaczyk A and Winterlich M 2006 *Phys. Rev. Lett.* **97** 135710
- [22] Noel T R, Parker R and Ring S G 2000 *Carbohydr. Res.* **329** 839
- [23] Molinero V and Goddard W A III 2005 *Phys. Rev. Lett.* **95** 045701
- [24] Kohlrausch R 1854 *Pogg. Ann. Phys.* **91** 179
- [25] Williams G and Watts D C 1970 *Trans. Faraday Soc.* **66** 80
- [26] Böhmer R, Ngai K L, Angell C A and Plazek D J 1993 *J. Chem. Phys.* **99** 4201
- [27] Döb A, Paluch M, Sillescu H and Hinze G 2002 *Phys. Rev. Lett.* **88** 095701
- [28] Ngai K L 2006 *J. Non-Cryst. Solids* **351** 2635
- [29] Ngai K L 1998 *J. Chem. Phys.* **109** 6982
- [30] Ngai K L and Capaccioli S 2004 *Phys. Rev. E* **69** 031501
- [31] Capaccioli S and Ngai K L 2005 *J. Phys. Chem. B* **109** 9727
- [32] Ngai K L, Casalini R, Capaccioli S, Paluch M and Roland C M 2005 *J. Phys. Chem. B* **109** 17356
- [33] Ngai K L, Casalini R, Capaccioli S, Paluch M and Roland C M 2006 *Adv. Chem. Phys. Part B* vol 133 (New York: Wiley and Son) chapter 10 pp 497–593
- [34] Paluch M, Casalini R, Hensel-Bielowka S and Roland C M 2002 *J. Chem. Phys.* **116** 9839
- [35] Hensel-Bielowka S, Paluch M and Ngai K L 2005 *J. Chem. Phys.* **123** 014502